284. On Excited States of Alkyl Bridged [14]Annulenes

by **Jens Spanget-Larsen** and **Rolf Gleiter**

Institut für Organische Chemie der Technischen Hochschule, D-6100 Darmstadt, BRD

(28.VIII.78)

Summary

The linear dichroic absorption spectrum of 1,3,6,8-*trans*-15,16-hexamethyldihydropyrene has been measured in stretched polyethylene at 77 K, and CNDO-CI calculations with inclusion of singly and doubly excited configurations have been carried out on a series of alkyl bridged [14]annulenes with pyrene- and anthracene-shaped perimeters. Transitions to $e_{3g} \rightarrow e_{4u}$ type ^1L and ^1B states are well described, and the results indicate that additional low-energy excited states originate from $e_{3g} \rightarrow e_{5g}$ and $e_{2u} \rightarrow e_{4u}$ type configurations interacting strongly with doubly excited configurations of the e_{3g}, $e_{3g} \rightarrow e_{4u}$, e_{4u} type. The second excited singlet state responsible for the weak transition observed between the ^1L bands may be assigned to one of these additional states, but it is probably of complex nature, similar to the 'phantom' state in linear polyenes.

Introduction. – The electronic structure of bridged annulenes has been the subject of several investigations, *e.g.* [1–8]. The electronic absorption spectra of these compounds are particularly interesting in that they provide a direct application of *Platt*'s classification of electronic states of cyclic polyenes [9], and they further offer the opportunity for studying the effects of distortions from planarity and inductive and hyperconjugative perturbations on the spectroscopic properties of conjugated π-electron systems.

The electronic absorption spectrum and polarized fluorescence of *trans*-15,16-dimethyl-dihydropyrene **1** *(Scheme 1)* and some of its simple derivatives were investigated some time ago by *Heilbronner et al.* [2], and the spectra of 1,6:8,13-cyclopropanediylidene[14]annulene (**2**), 1,6:8,13-ethanediylidene[14]annulene (**3**), 1,6:8,13-propane-1,3-diylidene[14]annulene (**4**), and 1,6:8,13-butane-1,4-diylidene[14]annulene (**5**) *(Scheme 1)* were studied recently by *Michl et al.* [7] by means of several experimental techniques, including linear dichroism in stretched polymer sheets. Characteristic absorption bands in the series of alkyl bridged [14]annulenes **1–5** could in all cases be assigned to L_b, L_a, B_b and B_a states derived from *Platt*'s perimeter model [9]. However, several additional[1]) transitions were observed. In par-

[1]) Throughout this paper, transitions other than L and B transitions will be termed 'additional'.

Scheme 1

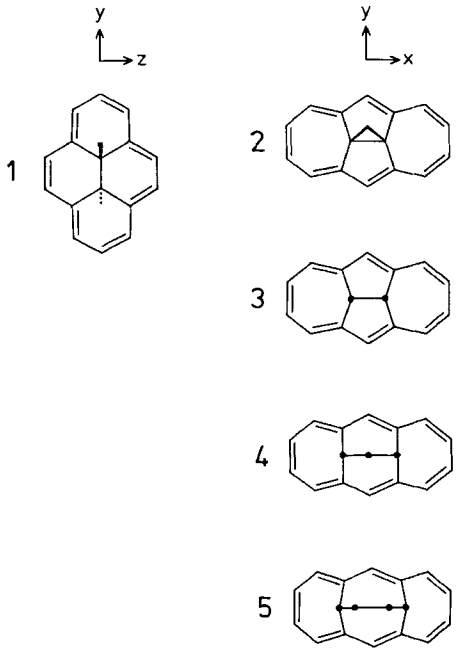

ticular, the existence of a very weak transition between the L_b and L_a bands indicates a fairly low-energy excited state which is not easily explained within the perimeter model. Calculations in the *Pariser-Parr-Pople* (PPP) [10] model on deformed and perturbed [14]annulenes gave no indication as to the assignment of this transition [2] [7]. *Michl et al.* [7] tentatively assigned this and 2 additional transitions at higher energy in the series **2–5** to partial charge-transfer transitions involving high-lying occupied σ-orbitals of the alkyl bridge and low-energy unoccupied orbitals of the π system.

In order further to characterize low-energy electronic transitions in **1–5** and possibly gain some insight into the origin of those apparently not predicted by the perimeter model, we have undertaken an investigation of these compounds. First, we measured the linear dichroic absorption spectrum of the 1,3,6,8-tetramethyl derivative of **1** in stretched polyethylene at 77 K. Second, we performed CNDO-CI calculations on **1–5** using a modified version of the computer program published by *Baumann* [11] with inclusion of singly and doubly excited configurations in the CI procedure. It will be shown that this model performs reasonably satisfactorily for these twisted π-systems, somewhat in contrast to expectations expressed previously [6] [7]. The results are in general agreement with the identification of L and B bands suggested [2] [7], but are at variance with the tentative assignment of the additional transitions [7].

Linear dichroism of 1,3,6,8-*trans*-15,16-hexamethyl-dihydropyrene. – The polarized absorption spectrum measured in stretched polyethylene at 77 K according to

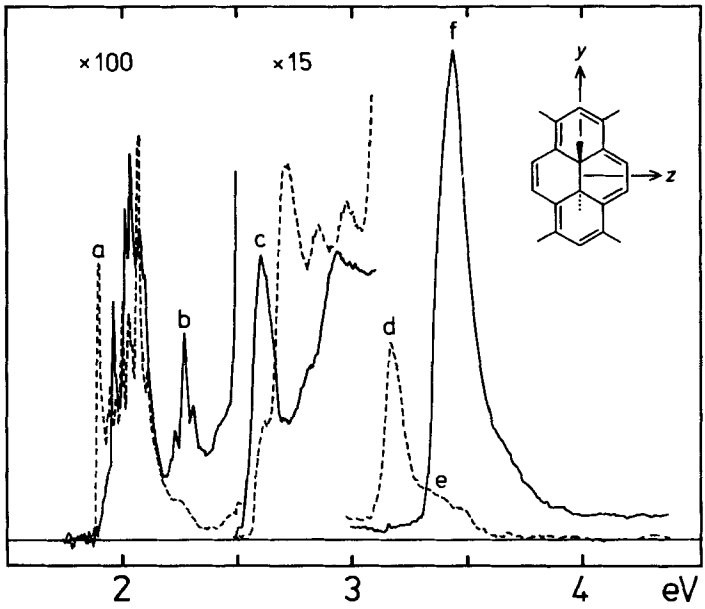

Fig. 1. *Polarized absorption spectrum of 1,3,6,8-*trans*-15,16-hexamethyldihydropyrene measured at 77 K in stretched polyethylene.* The *Figure* shows the reduced absorption curves $A_y = E_\parallel - 0.95 E_\perp$ (full line) and $A_z = 1.40\ [E_\perp - 0.55 E_\parallel]$ (broken line), where $E_\parallel$ and $E_\perp$ are the absorption curves measured with the stretching direction parallel and perpendicular to the plane of the linearly polarized light. The designation of axes deviates from that usually adopted in stretched sheet work [12] [16]. The labeling of peaks **a**–**f** refers to the labeling in [2].

the procedure of *Eggers et al.* [12] is shown in *Figure 1* (for experimental details, see [13–15]). The stretched sheet spectrum in the region above 2.5 eV has been determined at RT. by *Schmidt* [4]; the 2 spectra are essentially similar in that region, apart from improved resolution of the medium intense absorption between 2.5 and 3.0 eV in the low temperature spectrum. *Figure 1* shows the reduced absorption curves obtained from the experimental dichroic spectra using the reduction factors [12] $d^0_\parallel = 0.95$ and $d^0_\perp = 0.55$. These values were determined from the assumptions that the peak at 3.4 eV (**f**) and the peaks at 1.9 and 3.2 eV (**a** and **d**) are 'long' and 'short' axis polarized, respectively. The reduction factors correspond to the orientation factors [12] [16] $K_1 = 1/(2d^0_\perp + 1) = 0.48$, $K_2 = d^0_\parallel/(2 + d^0_\parallel) = 0.32$, and $K_3 = 1 - K_1 - K_2 = 0.20$. The orientation factors are quite similar to those for pyrene ($K_1 = 0.54$, $K_2 = 0.32$) [17]. The observation $K_2 > K_3$ indicates that 'short' axis polarized features such as **a** and **d** are polarized along the 'in-plane' z-axis rather than along the 'out-of-plane' x-axis, which is the axis least likely to align with the stretching direction.

The polarized absorption spectrum in *Figure 1* is consistent with the relative polarization directions of the main bands **a**, **c**, **d** and **f** as determined by polarized fluorescence of the 2-acetamido derivative of **1** [2]. The stretched sheet spectrum contains additional detail. Band **a** shows strongly mixed polarization (in contrast to the corresponding band in **2**–**5** [7]) and band **b** is predominantly 'long' axis polar-

ized. Between the bands **c** and **d** are observed at least 3 'short' axis polarized peaks and one 'long' axis polarized peak. The transition **e** appears as a poorly resolved 'short' axis polarized absorption overlapping the tail of band **d** and the onset of the very strong band **f**.

Calculations. – In the preliminary stages, some calculations were performed using *Del Bene & Jaffé*'s CNDO/S-CI [18] and *Krogh-Jespersen & Ratner*'s INDO/S-CI [19] methods with inclusion of singly excited configurations in the CI. Both methods predicted reasonably well the position of L and B bands for a compound such as **3**, but they did not predict any additional transitions below the B bands, irrespective of variation of geometry or extent of singly excited CI. However, as pointed out in [7], a large number of doubly excited configurations are present at relatively low energies. and we decided to use *Baumann*'s CNDO/S-CI program [11] which includes these configurations.

The original CDC-version of this program [11] was modified to conform to IBM standards; during this procedure some errors were corrected. The calculations were performed with inclusion of the 49 singly excited singlet configurations derived by promotion from the 7 highest occupied into the 7 lowest unoccupied orbitals, as well as the 45 doubly excited singlet configurations derived by excitation from the 3 highest occupied to the 3 lowest unoccupied orbitals. This is a significant extension of the CI relative to the calculations referred to above, but it is still very limited, considering the size of the compounds **1–5**, and the selection of configurations is quite arbitrary. We feel, however, that calculations at this level should give a first indication of possible assignments of low-energy transitions in these species, since it is unlikely that extension or optimization of the CI expansion introduces completely new transitions below, say, 4 eV. The original parameters stored in the program were applied [11], except for the β values for

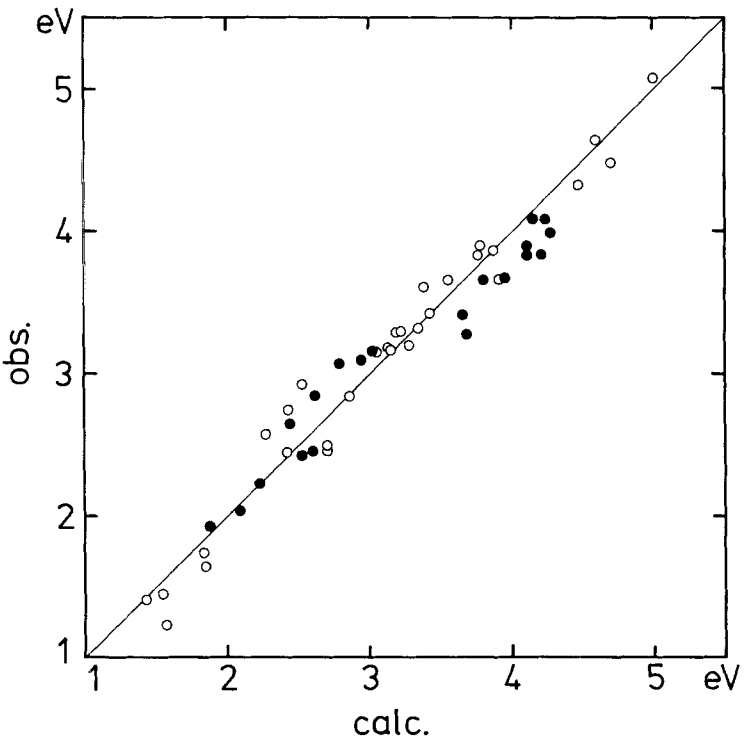

Fig.2. *Correlation of observed and calculated transition energies for* **1–5** (solid points) *and* **6–11** (open points)

carbon and hydrogen which were taken as $\beta^0_C = -15.0$ eV and $\beta^0_H = -10.0$ eV (1 eV $\approx$ 96.487 kJ/mol $\approx$ 8068 cm^{-1}). Furthermore, carbon 2*s*-2*p* contributions to electric dipole transition moments were included according to

$$\langle 2s|\vec{r}|2p_z\rangle = 5/2\zeta\sqrt{3} \text{ (a.u.)} \quad (1)$$

where ζ is the *Slater* exponent. These contributions might be important in calculation of intensities of σ-π type transitions.

The procedure was tested by its ability to reproduce singlet-singlet transitions in the planar π-electron systems pleiadene **6** [20], azuleno(1,2,3-*cd*)phenalene **7** [15], azuleno(5,6,7-*cd*)phenalene **8** [21], aceheptylene **9** [14], dicyclohepta[*cd,gh*]pentalene **10** [22], and pyrene **11** [17] *(Scheme 2)*. In the case of **6**, **7** and **8** idealized 'regular' geometries with all C–C distances equal to 140 pm were employed. For **9** and **10** structures estimated by *Lindner* [23] were used, while for **11** the experimental geometry [24] was taken. *Figure 2* shows the linear regression of observed energies for 30 selected transitions in **6**–**11** on the corresponding calculated ones (open points). Only transitions for which the assignment based on experimental criteria and the results of PPP-type and other calculations is well established, were included in the correlation. The β^0_C and β^0_H parameters were adjusted to obtain a regression line with slope equal to unity (see above); the standard deviation is 0.17 eV (1400 cm^{-1}) and no deviations are larger than 0.4 eV (3400 cm^{-1}). These results are reasonably satisfactory, but not better than corresponding PPP-results [14] [15] [17] [20–22]. It is particularly important that the calculations reproduce low-energy states in **6** and **7** which depend strongly on doubly excited configurations in the CI description [15] [20] (see *Table 1*). This indicates that the method is adequately parametrized for a description of such states in π-electron systems of a size comparable to those of **1–5**.

As a further test of the applicability of the method, we have compared observed ionization energies and calculated orbital energies (*Koopmans'* theorem [25]). In the calculations on the bridged [14]annulenes we used geometries derived from experimental X-ray data for **1** [26], **4** [27], and **5** [28], while the results for **2** and **3** were based on geometries calculated by *Lindner*'s combined force field and π-SCF-LCAO-MO method [23] which yields results in close agreement with experiment [29] [30]. The results displayed in *Figure 3* indicate that the calculated orbital energies are in excellent agreement with the shifts and relative spacing of the lowest few ionization energies as measured by photoelectron spectroscopy [5] [6]. The only discrepancy concerns the third level of **1** (a_u) which is predicted at relatively high

Table 1. *Observed and calculated transition energies* E (eV), *polarization directions, and log ε values for pleiadene* **6** *and azuleno(1,2,3-*cd*)phenalene* **7**

	Obs.			Calc.		
	E	pol.	log ε	*E*	pol.	log ε[a])
6[b])	1.45	*y*	~3	1.55	*y*	3.3
	2.46	*z*	~2	2.42[c])	*z*	3.0
	2.85	*z*	~4	2.86	*z*	4.1
				2.89	*y*	2.4
	3.29	*y*	3.8	3.19	*y*	3.7
	3.61	*z*	3.6	3.38	*z*	3.1
7[d])	1.41	*y*	2.5	1.43	*y*	2.4
	2.58	*z*	4.7	2.27	*z*	4.0
	3.17	*z*	3.9	3.15[e])	*z*	3.4
	3.3	*y*	-	3.22	*y*	3.1
				3.40	*y*	1.5
	3.43	*z*	4.9	3.42	*z*	4.6

[a]) Estimated by the relation $\log \varepsilon = 4.74 + \log f$ [11].
[b]) Observed band origins from [20].
[c]) 67% doubly excited character.
[d]) Observed band maxima from [15].
[e]) 31% doubly excited character.

Scheme 2

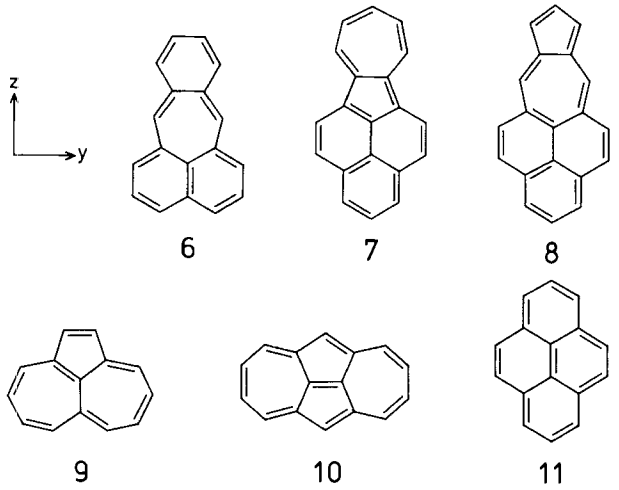

binding energies. The predicted ordering is in agreement with the original assignments [5] [6] except for the ordering of the closely spaced 2 first levels in **10**, **2** and **3**; however, the ordering indicated in *Figure 3* is consistent with the results of other all-valence-electrons calculations [8] [31].

All things considered, the results indicate that the procedure outlined in this section is applicable to the electronic structure of the annulenes **1–5**. Results for excited states of these compounds are discussed in the following.

Results and discussion. – Observed calculated transitions for **1–5** are given in *Table 2*, and the correlation of the most important transitions is indicated in *Figure 4*. The experimental data are taken from *Heilbronner et al.* [2] (**1**) and *Michl et al.* [7] (**2–5**). The polarization directions for **1** are inferred from the stretched sheet spectrum of the methyl derivative in *Figure 1*.

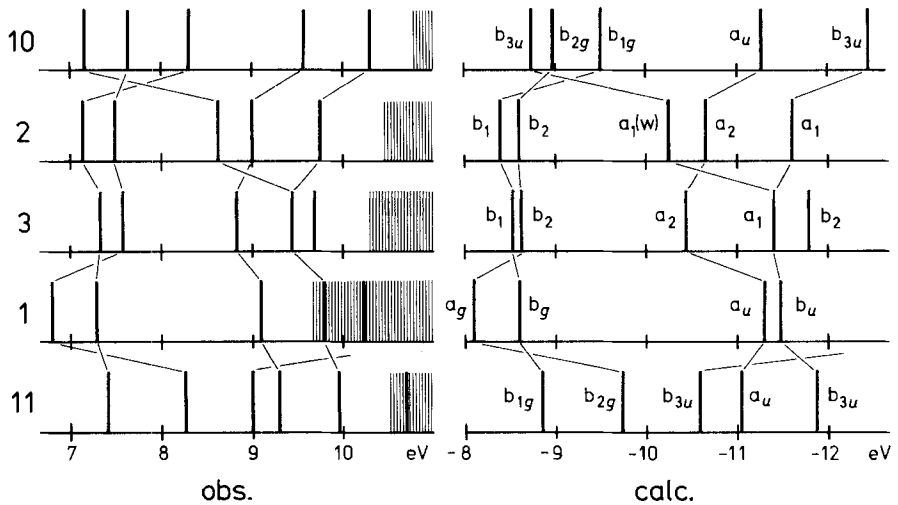

Fig. 3. *Observed ionization energies* (left) *and calculated orbital energies* (right) *for* **10**, **2**, **3**, **1**, *and* **11**

Table 2. *Observed and calculated singlet transition energies* E (eV), *polarization directions, and oscillator strengths f for the alkyl bridged [14]annulenes* **1–5**

		Obs.			Calc.		
		E	pol.	f	*E*	pol.	f
1[a])	L_b	1.93	*z*	0.002	1.88	*z*	0.014
		2.34	(*y*)	~0.0002			
	L_a	2.65	*y*	0.085	2.44	~*y*	0.006
					3.10[b])	–	–
					3.25[c])	–	–
					3.59[c])	–	–
	B_b	3.28	*z*	0.20	3.68	*z*	0.53
		3.51	*z*	~0.1	3.70[c])	–	–
					3.79[c])	–	–
	B_a	3.67	*y*	0.68	3.95	~*y*	1.19
2[d])	L_b	2.04	*x*	0.013	2.09	*x*	0.022
		2.45	(*x*)	0.0003			
	L_a	2.85	*y* or *z*	0.008	2.61	*y*	0.006
		3.04	*y* or *z*	0.03	3.48[b])	*z*	0.010
		3.12	*x*	0.03	3.51[b])	–	–
					3.61[b])	*z*	0.003
	B_a	3.41	*y* or *z*	0.13	3.65	*y*	0.48
					3.80	–	–
					3.97[c])	*z*	0.004
					4.15[b])	*z*	0.005
	B_b	3.84	*x*	1.3	4.21	*x*	1.49
3[d])	L_b	2.23	*x*	0.020	2.23	*x*	0.018
		2.64	(*x*)	0.0004			
	L_a	3.07	*y* or *z*	0.02	2.79	*y*	0.031
		3.25	*x*	0.08	3.46[b])	–	–
		3.35	*y* or *z*		3.72[b])	*z*	0.004
					3.78[c])	*z*	0.0004
	B_a	3.66	*y* or *z*	0.15	3.80	*y*	0.39
					3.97[c])	–	–
					4.20[c])	*z*	0.004
	B_b	3.99	*x*	1.1	4.27	*x*	1.49
4[d])	L_b	2.43	*x*	0.004	2.53	*x*	0.007
		2.80	(*x*)	0.0001			
	L_a	3.1	*y* or *z*	0.06	2.94	*y*	0.037
		3.41	*x*	0.09	3.55[b])	–	–
		3.6 (?)	*y* or *z*	~0	3.73[b])	*z*	0.0009
					3.99[c])	*z*	0.0001
	B_a	3.85	*y* or *z*	0.15	4.12	*y*	0.28
					4.24	–	–
	B_b	4.09	*x*	1.6	4.24	*x*	1.23
5[d])	L_b	2.46	*x*	0.003	2.60	*x*	0.001
		2.83	(*x*)	0.0002			
	L_a	3.16	*y* or *z*	0.04	3.02	*y*	0.012
		3.47	*x*	0.11	3.60	*z*	~0
		3.66 (?)	*y* or *z*	~0	3.66[b])	–	–
	B_a	3.90	*y* or *z*	0.21	4.11	*y*	0.27
	B_b	4.09	*x*	1.2	4.15	*x*	1.01

[a]) Observed band maxima from [2], polarized directions inferred from the spectrum in *Figure 1.*
[b]) More than 20% doubly excited character.
[c]) More than 50% doubly excited character.
[d]) Observed band origins from [7].

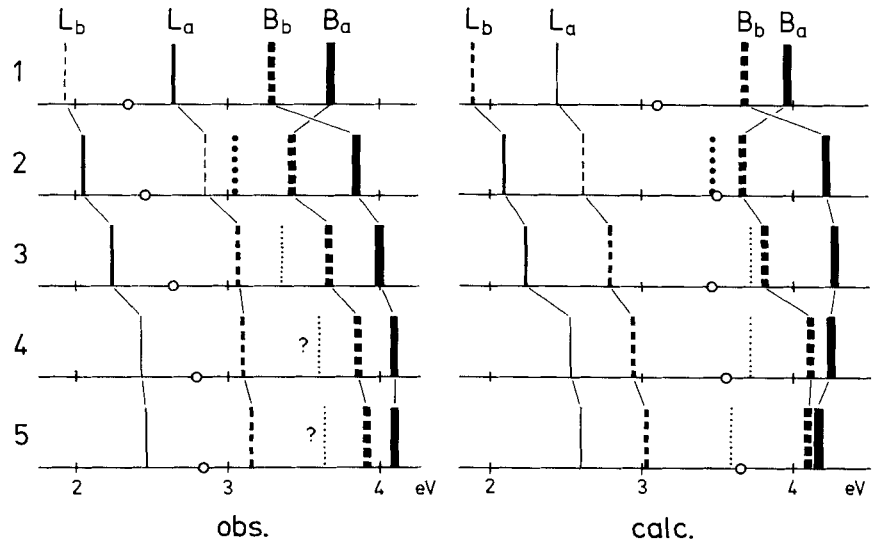

Fig. 4. *Observed* (left) *and calculated* (right) *transition energies for the alkyl bridged [14]annulenes* **1–5**. Solid and broken bars indicate 'long-axis' and 'short-axis' polarized transitions, respectively; dotted bars indicate transitions which are predicted to be 'out-of-plane' z-axis polarized in **2–5**. The thickness of the bars indicates very weak ($f < 0.01$), weak ($0.01 < f < 0.1$), and medium to intense ($f > 0.1$) transitions; transitions which are predicted to be forbidden by symmetry are indicated by circles. Not all calculated transitions are shown *(cf. Table 2)*.

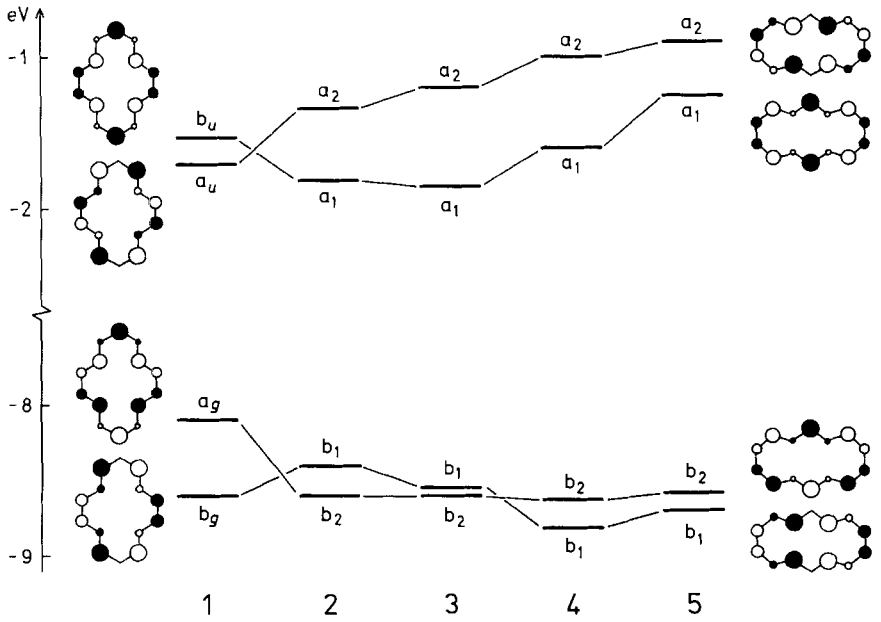

Fig. 5. *Calculated* e_{3g} *and* e_{4u} *frontier orbitals for* **1–5** *(cf. Scheme 3)*

L and B transitions according to *Platt* [9] correspond to excitation of an electron from the 2 highest occupied to the 2 lowest unoccupied perimeter π-orbitals, as indicated in *Figure 5*. These 'frontier' orbitals have e_{3g} and e_{4u} symmetry, respectively, in an unperturbed D_{14h} [14]annulene, where they are completely determined by symmetry. The symmetry is reduced to C_{2h} in the bridged [14]annulene **1** and to C_{2v} in **2–5** *(Scheme 3)*. The splitting of the e_{3g} and e_{4u} type orbitals in these compounds can be explained in terms of the effects of twisting and non-planarity of the perimeter and 'through-space' and 'through-bond' *trans*annular interactions [1–3] [5–8]. The present results predict a reversal in the order of the 2 highest occupied b_1 and b_2 orbitals in the series **2–5**; this is due to interaction of the b_1 orbital with an occupied σ orbital of the bridge in the case of **2** and **3**. In **2** this σ orbital is the w (A) *Walsh*-type orbital of the cyclopropane ring, in **3** a closely related ethane orbital with C–C *anti*-bonding and C–H bonding characteristics (1 e″ in eclipsed ethane [32]). No equivalent orbitals are available in the propano- and butano-bridged compounds **4** and **5**. Similar results were obtained with the extended *Hückel* method [8].

The calculated 'frontier' orbital gap increases through the series **1–5**, which is consistent with the observed shift of the L and B transitions towards higher energies. For compounds **2–5**, *Michl et al.* [7] explained this trend as due to an increasingly dominating *trans*annular homo-conjugative interaction. The orbital shifts from **1** to **2** and **3** are largely due to the different topologies, which cause the σ-orbitals of the alkyl bridge to interact with different perimeter π-orbitals. A high-lying occupied σ-orbital of the butane bridge in **1** interacts quite strongly with the highest occupied a_g perimeter orbital, leading to a very low first ionization energy (observed value 6.8 eV) [5] and low L and B transition energies *(Fig. 3* and *4)*.

The calculated L_b, L_a, B_b and B_a transitions compare well with the experimental data. The correlation of observed [2] [7] and calculated transition energies is indicated in *Figure 2* (solid points); it is seen that the scatter of the points is comparable to that for points relating to π-π^* transitions in planar hydrocarbons (open points). The L_b transitions which correspond to the first band in each spectrum are particularly well reproduced. The energy is predicted to within a few hundredths of an eV and the variation of the oscillator strength in the series **1–5** is quite well reproduced, as shown in *Figure 6*. The L_a transitions are generally predicted at slightly too low energies, and the correlation of observed and calculated oscillator strengths is less convincing. In particular, the intensity of the L_a band of **1** (corresponding to band **c** in *Fig. 1*) is grossly underestimated. However, the experimental determination of oscillator strengths for these transitions is complicated by overlapping bands, and contributions, due to vibronic coupling with the much stronger B bands are probably significant; a similar conclusion was reached by *Heilbronner et al.* [2].

The results suggest a minor reassignment of the L_a band in the case of **2**, relative to the assignment suggested by *Michl et al.* [7]. Correlation of results in the series **1–5** favours assignment of the peak at 2.85 eV in the spectrum of **2** to the L_a transition, rather than the peak at 3.04 eV *(Table 2, Fig. 4)*. Within this assignment, the L_b and L_a bands are in all cases shifted similarly, except when going from **3** to **4** where the shift of the L_b band is much larger than that of the L_a band, as predicted by the calculation. This assignment is furthermore consistent with the predicted relative intensities of the L_b and L_a transitions for **2** *(e.g., Fig. 6)*.

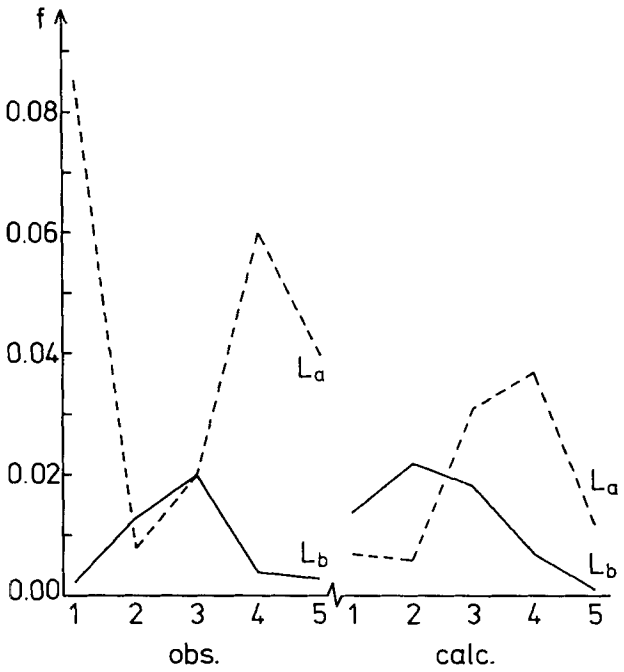

Fig. 6. *Observed* (left) *and calculated* (right) *oscillator strengths f for* L_b (solid line) *and* L_a (broken line) *in* **1–5**

The calculations predict several additional excited states below the B states. These states involve singly excited configurations of the $e_{3g} \rightarrow e_{5g}$ and $e_{2u} \rightarrow e_{4u}$ type and doubly excited configurations of the e_{3g}, $e_{3g} \rightarrow e_{4u}$, e_{4u} type *(Scheme 3)*. This group contains 8 singly excited and 10 doubly excited configurations with energies between 4 and 6 eV; they have A_g and B_g symmetry in the C_{2h} compound **1** and A_1 and A_2 symmetry in the C_{2v} compounds **2–5**. Transitions from the ground state to states derived from these configurations are all forbidden by symmetry, except for transitions to A_1 states in **2–5** which are polarized along the 'out-of-plane' *z*-axis. The interaction between singly and doubly excited configurations is very significant; this interaction is responsible for the prediction of additional states below the B

Scheme 3

	D_{14h}	C_{2h}		C_{2v}	
		Axis 'out-of-plane'	Axis 'in-plane'	Axis 'out-of-plane'	Axis 'in-plane'
—— ——	e_{5g}	b_g, b_g	a_g, b_g	b_2, b_1	a_2, b_1
—— ——	e_{4u}	a_u, a_u	b_u, a_u	a_1, a_2	a_2, b_1
—‖— —‖—	e_{3g}	b_g, b_g	a_g, b_g	b_2, b_1	b_1, a_2
—‖— —‖—	e_{2u}	a_u, a_u	b_u, a_u	a_1, a_2	b_1, a_2
			(**1**)	(**2–5**)	(**12**)

states, as shown in *Figure 7*. The large shift of the A_g (A_1) and B_g (A_2) states relative to the L and B states on inclusion of doubly excited configurations in the CI is largely due to the fact that the e_{3g}, $e_{3g} \rightarrow e_{4u}$, e_{4u} type configurations interact strongly with the former states but are prevented by symmetry from interaction with the latter; the L and B states mix only with higher configurations of A_u (B_1) and B_u (B_2) symmetry. This symmetry restriction applies to the unperturbed D_{14h} [14]annulene itself and to all perturbed systems which maintain inversion symmetry and/or the 'out-of-plane' C_2 axis. A different situation is represented by cyclopenta[*h*]cycl-[4.2.2]azine **12** which can be considered as a perturbed planar [14]annulene deformed to C_{2v} symmetry with the C_2 axis 'in-plane' [13]. In this case, all types of single and double promotions between perimeter π orbitals lead to configurations of A_1 and B_2 symmetry *(cf. Scheme 3)* and the symmetry restriction indicated above for **1–5** does not apply to **12**. Inclusion of doubly excited configurations in CNDO-CI calculations on **12** did *not* lead to the prediction of additional states below the B states, indicating that the symmetry restriction is crucial for the results in the case of **1–5**.

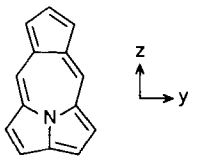

12

It is interesting to estimate the role of the bridging alkyl group and the various perturbations of the perimeter in the prediction of low energy additional states in **1–5**. We have performed a few calculations on a regular D_{14h} [14]annulene with

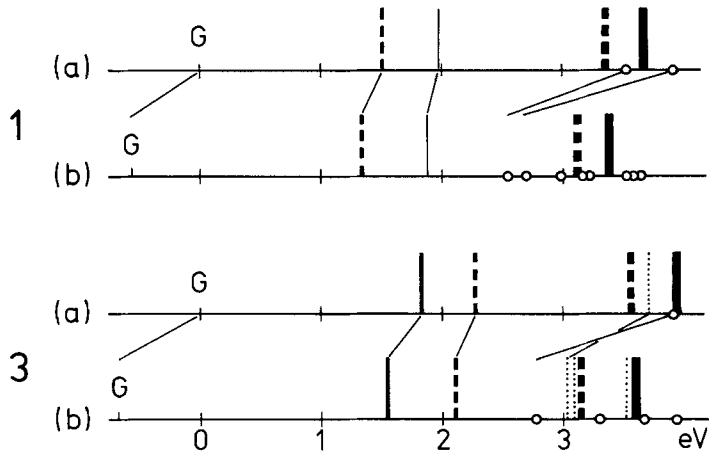

Fig. 7. *Calculated results for* **1** *and* **3**, (a) *with inclusion of singly excited configurations only, and* (b) *with inclusion also of doubly excited configurations* (G indicates the ground state; for remaining symbolism, see legend to *Fig. 4*)

C–C and C–H distances equal to 140 and 110 pm, respectively. Inclusion of doubly excited configurations in the CI introduced at least 2 doubly degenerate states between the L and B states. A calculation including 42 singly excited and 56 doubly excited configurations below 10 eV thus predicted B_{2u} (L_b) and B_{1u} (L_a) states at 2.05 and 2.62 eV, respectively, E_{2g}(C) and E_{6g}(K) states at 3.95 and 4.04 eV, respectively, and the E_{1u}(B) state at 4.32 eV. Hence, within the model and the parametrization applied, perturbation of the [14]annulene due to twisting, non-planarity, or *trans*-annular and hyperconjugative interactions is not essential in bringing down additional states below the B states. On the other hand, these interactions may further lower the energy of these states. In particular, interaction with σ-orbitals tend to destabilize the e_{2u} type orbitals, thereby lowering the energy of $e_{2u} \rightarrow e_{4u}$ type configurations, leading to further stabilization of states in **1–5** involving these configurations. These states are influenced to some extent by σ-π mixing, but inspection of the calculated wave functions indicates that it would be misleading to characterize transitions to these states as σ-π^* or charge-transfer transitions in the sense implied by *Michl et al.* [7], since the partial charge transfer from the alkyl bridge to the π system is insignificant (see later an exception in the case of **2**).

Additional low-energy transitions in **1–5** are thus predicted to be characteristic for the [14]annulene chromophore, rather than transitions depending on the presence of the saturated bridge. The basic mechanism which leads to the prediction of low-energy additional states is similar to the one which leads to reversal of the 2 lowest excited singlet states of *trans*-polyenes when doubly excited configurations are included in the CI [33]. The π orbitals of a C_{2h} *trans*-polyene have alternatingly a_u and b_g symmetry. Transition from the highest occupied to the lowest unoccupied orbital is allowed and gives rise to a B_u state which is related to the B states of the cyclic polyene. Strong interaction between the next-lowest singly and lowest doubly excited configurations predicts a low-energy excited A_g state which is believed to correspond to the 'phantom' state observed below the B_u state in some *trans*-polyene derivatives [33] [34]. The prediction of similar low-energy states for [14]annulenes is a reflection of the close correspondence between the electronic structures of linear and cyclic polyenes [35] and indicates that the low-energy 'phantom' states observed for both classes of compounds may be closely related.

We believe that the additional transitions observed in **1–5** must involve states of the type discussed above, at least in case of the weak transition observed between the L_b and L_a bands. In any case, no other calculated transitions come near this region. This transition is clearly seen in the spectrum in *Figure 1* (**b**) and in the spectra of **2** and **3**, but overlaps strongly with the tail of the L_b band in case of **4** and **5** [7]. The calculated transition energy is at least 0.7–1.0 eV too high *(Table 2, Fig. 4);* variation of parameters and extension of the CI did not remove this discrepancy. *Leclercq & Leclercq* [33] had similar problems in reproducing the 'phantom' A_g state of diphenyl-*trans*-polyenes in spite of very extensive CI calculations. They concluded that the 'phantom' state may not have pure-valence character. It cannot be excluded that the second excited singlet state in **1–5** is of similar complex nature. The calculated results indicate that it has A_g or B_g symmetry in **1** and A_1 or A_2 symmetry in **2–5**, implying that the predominantly 'long' axis polarized intensity of the observed absorption band is not intrinsic but borrowed from much more intense

neighbouring transitions by vibronic interactions. A similar state is not predicted for **12**, as discussed above. Unfortunately, the absorption spectrum of **12** [13] does not allow any conclusion concerning the existence of a weak transition corresponding to transition **b** in *Figure 1*. Definitive assignment and characterization of this extremely interesting state of **1–5** must await the results of further investigations.

The spectral region between the L and B bands of **1–5** is complicated, as clearly demonstrated by the region between the peaks **c** and **d** in *Figure 1*. Assignment of bands in this region to the several transitions predicted between 3 and 4 eV is difficult and is probably complicated by strong vibronic interaction with the intense B bands. We therefore refrain from further consideration of this spectral region, apart from the possible assignment of the fairly intense 'short' axis polarized transition observed at 3.04 eV in the spectrum of **2**, close to the weaker L_a band at 2.85 (our assignment). The transition is indicated by a dotted bar in *Figure 4*. The calculated results indicate that this absorption can be assigned to an 'out-of-plane' z-polarized transition to a totally symmetric state predicted at 3.47 eV *(Table 2)*. This transition is predicted to be more intense than the 'in-plane' y-polarized L_a transition; this result is independent of the inclusion of one-center s–p contributions (1) to the transition moment. The excited state is fairly well described by the configuration derived by promotion of an electron from the third highest occupied orbital $a_1(w)$ *(Fig. 3)* to the lowest unoccupied e_{4u}-type orbital $a_1(\pi^*)$ *(Fig. 5)*. The $a_1(w)$ orbital is the result of strong interaction between the w(S) *Walsh*-type orbital of the cyclopropane ring and the appropriate component of the e_{2u}-type perimeter π-orbital; the *Walsh*-orbital character is 61%. Related transitions to low-energy A_1 states are predicted in **3**, **4** and **5**, but with strongly decreasing intensity through the series **2–5**, in fairly good agreement with experiment [7] *(Table 2, Fig. 4)*.

We shall conclude with a few remarks on the MCD. (magnetic circular dichroism) [36] B-terms for the lowest transitions in **1–5**. *Michl* [37] has derived a simple rule

$$\text{sign } B = \text{sign } (\Delta\text{HOMO} - \Delta\text{LUMO}) \tag{2}$$

relating the sign of the lowest π-π^* B-term in a perturbed [4n+2]annulene to the energy difference between the 2 highest occupied π orbitals (ΔHOMO) and that of the 2 lowest unoccupied π orbitals (ΔLUMO). It is then clear by inspection of *Figure 5* that the lowest B-term is predicted to be positive for **1** and negative for **2–5**. This is in agreement with the observed MCD. spectra for **2–5** [7]; indeed, not only sign but also variation of magnitude of the B-term for the L_b transition is well predicted by the quantity ΔHOMO – ΔLUMO (observed lowest B-term for **2–5** is -0.3, -0.6, -0.4, and -0.1, respectively, in units of $10^{-3}\beta_e$ D^2/cm^{-1}; the corresponding value of ΔHOMO – ΔLUMO is -0.30, -0.60, -0.41, and -0.23 eV). If the B-term for the L_a transition is dominated by magnetic coupling with the L_b transition, then its sign should be opposite to that of the L_b transition, *i.e.* positive in **2–5**. This is in agreement with the observed signs, except in the case of **2** where the L_a band at 2.85 eV has a negative B-term, and the stronger peak at 3.04 eV a positive B-term [7]. This was one reason why *Michl et al.* assigned the latter peak to the L_a transition. However, the B-term for the peak at 2.85 eV is probably dominated by coupling

with the neighbouring transition at 3.04 eV which is much closer in energy and much more intense than the L_b transition *(Table 2)*. According to our assignment, the 2 peaks at 2.85 and 3.04 eV are polarized in mutually perpendicular directions, along the 'in-plane' *y*-axis and the 'out-of-plane' *z*-axis, allowing for strong magnetic coupling. An analysis of MCD. B-terms for the three-dimensional chromophore **2** would probably be rewarding.

Conclusion. – The most important results of this investigation can be summarized as follows:

a) CNDO-CI theory performs reasonably satisfactorily for L and B transitions in bridged [14]annulenes, even within a limited CI. The results for additional transitions depend strongly on the extension of the CI expansion, particularly on the inclusion of doubly excited configurations.

b) Prediction of the second excited singlet state responsible for the weak transition observed between the L bands is not straightforward. It probably involves several strongly interacting $e_{3g} \rightarrow e_{5g}$, $e_{2u} \rightarrow e_{4u}$, and e_{3g}, $e_{3g} \rightarrow e_{4u}$, e_{4u} type configurations and may correspond to the 'phantom' state in linear polyenes.

c) A fairly intense 'out-of-plane' polarized transition is predicted for **2**, involving partial charge transfer from an occupied *Walsh* orbital of the cyclopropane bridge to the lowest π^* orbital of the perimeter.

We are grateful to Prof. Dr. *V. Boekelheide* for the gift of a sample of 1,3,6,8-*trans*-15,16-hexamethyl-dihydropyrene, to Dr. *H.F. Baumann* for providing a card deck of his CNDO-CI program, and to Dr. *K. Krogh-Jespersen* for performing INDO/S-CI calculations on the compounds **3** and **10**. Financial support by the *Deutsche Forschungsgemeinschaft* and the *Fonds der Chemischen Industrie* is gratefully acknowledged.

REFERENCES

[1] *H.-R. Blattmann, W.A. Böll, E. Heilbronner, G. Hohlneicher, E. Vogel & J.-P. Weber,* Helv. *49,* 2017 (1966).
[2] *H.-R. Blattmann, V. Boekelheide, E. Heilbronner & J.-P. Weber,* Helv. *50,* 68 (1967).
[3] *W. Grimme, E. Heilbronner, G. Hohlneicher, E. Vogel & J.-P. Weber,* Helv. *51,* 225 (1968).
[4] *D. Schmidt,* Diss. ETH Zürich, Nr. 4517, 1970.
[5] *V. Boekelheide, J.N. Murrell & W. Schmidt,* Tetrahedron Letters *1972,* 575; *R. Boschi & W. Schmidt, ibid. 1972,* 2577.
[6] *C. Batich, E. Heilbronner & E. Vogel,* Helv. *57,* 2288 (1974).
[7] *J. Kolc, J. Michl & E. Vogel,* J. Amer. chem. Soc. *98,* 3935 (1976).
[8] *A. Gavezzotti & M. Simonetta,* Helv. *59,* 2984 (1976).
[9] *J.R. Platt,* J. chem. Physics *17,* 484 (1949); *W. Moffit, ibid. 22,* 320 (1954).
[10] *R. Pariser & R.G. Parr,* J. chem. Physics *21,* 466, 767 (1953); *J.A. Pople,* Trans. Faraday Soc. *49,* 1375 (1953).
[11] *H. Baumann,* QCPE *10,* 333 (1977).
[12] *E.W. Thulstrup, J. Michl & J.H. Eggers,* J. phys. Chemistry *74,* 3868 (1970); *J. Michl, E.W. Thulstrup & J.H. Eggers, ibid. 74,* 3878 (1970).
[13] *J. Spanget-Larsen, R. Gleiter, R. Haider & E.W. Thulstrup,* Mol. Physics *34,* 1049 (1977).
[14] *P. Bischof, R. Gleiter, K. Hafner, M. Kobayashi & J. Spanget-Larsen,* Ber. Bunsenges. physik. Chem. *80,* 532 (1976).
[15] *R. Gleiter, J. Spanget-Larsen, E.W. Thulstrup, I. Murata, K. Nakasuji & C. Jutz,* Helv. *59,* 1459 (1976).
[16] *J. Michl & E.W. Thulstrup,* Spectroscopy Letters *10,* 401 (1977).

[17] *E. W. Thulstrup, J. W. Downing & J. Michl,* Chem. Physics *23,* 307 (1977).
[18] *J. Del Bene & H. H. Jaffé,* J. chem. Physics *48,* 1807 (1968); *J. Del Bene, H. H. Jaffé, R. L. Ellis & G. Kuehnlenz,* QCPE *9,* 174, 1970.
[19] *K. Krogh-Jespersen & M. Ratner,* J. chem. Physics. *65,* 1305 (1976); Theoret. chim. Acta (Berl.) *47,* 283 (1978).
[20] *J. Kolc, J. W. Downing, A. P. Manzara & J. Michl,* J. Amer. chem. Soc. *98,* 930 (1976).
[21] *E. W. Thulstrup, J. Michl & C. Jutz,* J. chem. Soc. Faraday II *71,* 1618 (1975).
[22] *V. Kratochvíl, J. Kolc & J. Michl,* J. mol. Spectrosc. *57,* 436 (1975).
[23] *H. J. Lindner,* Tetrahedron *30,* 1127 (1974).
[24] *A. C. Hazell, F. K. Larsen & M. S. Lehmann,* Acta crystallogr. *B28,* 2977 (1972).
[25] *T. Koopmans,* Physica *1,* 104 (1934).
[26] *A. W. Hanson,* Acta crystallogr. *18,* 599 (1965).
[27] *A. Gavezzotti, A. Mugnole, M. Raimondi & M. Simonetta,* J. chem. Soc. Perkin II, *1972,* 425.
[28] *C. M. Gramaccioli, A. Mugnoli, T. Pilati, M. Raimondi & M. Simonetta,* Acta crystallogr. *B28,* 2365 (1972).
[29] *A. Mugnoli & M. Simonetta,* Acta crystallogr. *B30,* 2896 (1974).
[30] *R. Bianchi, G. Casalone & M. Simonetta,* Acta crystallogr. *B31,* 1207 (1975).
[31] *P. Bischof & R. Gleiter,* in 'Topics in Nonbenzenoid Aromatic Chemistry', Vol. II, T. Nozoe et al., ed., Hirokawa Publishing Company, Tokyo 1977.
[32] *W. L. Jorgensen & L. Salem,* 'The Organic Chemist's Book of Orbitals', Academic Press, New York 1973.
[33] *J. Leclercq & J. M. Leclercq,* Chem. Physics Letters *57,* 54 (1978), and Ref. therein.
[34] *H. L.-B. Fang, R. J. Trash & G. E. Leroi,* Chem. Physics Letters *57,* 59 (1978), and Ref. therein.
[35] See *e.g., E. Heilbronner & H. Bock,* «Das HMO-Modell und seine Anwendung», Verlag Chemie, Weinheim Bergstr. 1968.
[36] For an introduction to the MCD. Spectroscopy of hydrocarbon π systems, see J. Michl, Int. J. Quant. Chemistry (S) *10,* 107 (1976).
[37] *J. Michl,* Chem. Physics Letters *43,* 457 (1976).

285. Stereochemie der Bildung und Spaltung der (Co–C)-Bindung an einem Vitamin-B_{12}-Modell

3. (vorläufige) Mitteilung[1])

von **Lorenz Walder, Gerhard Rytz, Kurt Meier** und **Rolf Scheffold**

Institut für organische Chemie der Universität Bern, Freiestrasse 3, CH-3012 Bern

(8. XI. 78)

Stereochemical Course of the Formation and Cleavage of the Co–C Bond in a Vitamin B_{12} Model

Summary

The electrosynthesis and properties of a chiral cobalt alkyl complex **4** are described. The reductive cleavage of the Co–C bond occurs with retention of configuration at the C-atom.

[1]) 2. Mitt.: «Über Synthese und Reaktionen von Metallkomplexen mit porphinoidem Ligandsystem», s. [1].